

Single electron pumping through a quantum dot-embedded carbon nanotube using surface acoustic wave

Bum-Kyu Kim,^{1,2} Ju-Jin Kim,² Minky Seo,³ Yunchul Chung,³ Byung Chil Woo,¹ Jinhee Kim,¹ Woon Song,¹ and Nam Kim^{1,a)}

¹Division of Convergence Technology, Korea Research Institute of Standards and Science, Daejeon 305-600, Republic of Korea

²Department of Physics, Chonbuk National University, Jeonju 561-756, Republic of Korea

³Department of Physics, Pusan National University, Busan 609-735, Republic of Korea

(Received 1 October 2010; accepted 8 December 2010; published online 29 December 2010)

We have studied acoustoelectric current through a quantum dot-embedded carbon nanotube induced by a surface acoustic wave. The measurements were carried out on a same device but in two very different quantum dot charging energy E_c regimes (~ 50 and ~ 5 meV). The results showed dramatic differences in induced acoustoelectric current depending on E_c . The induced acoustoelectric current showed a polarity reversal around the Coulomb blockade peak when E_c is small (5 meV). For a large E_c (50 meV), however, a current plateau was observed as a function of surface acoustic wave powers as well as gate voltages. © 2010 American Institute of Physics. [doi:10.1063/1.3532852]

Recently, there have been numerous efforts to establish a quantum current standard based on a solid-state device. Most of the devices have exploited the quantization of current through a one-dimensional (1D) conduction wire driven by surface acoustic wave (SAW) propagating along the wire.¹ When SAW is applied along a 1D wire, the superposition of the SAW and 1D potential forms moving quantum dots on the wire. Each quantum dot carries an integer number of electron n at the rate of SAW frequency f . Hence, the induced current I becomes $I = nef$ where n and e are integer number and electron charge, respectively. Typically, quantum point contact (QPC) structure from a two-dimensional (2D) electron gas was used as a 1D wire in the previous studies. Recently, there have been a few efforts to substitute QPC with a single-walled carbon nanotube (CNT), an ideal 1D wire.²⁻⁷ Adiabatic charge pumping in CNT quantum dots (QDs),³ and the observation of current quantization in a semiconducting single-walled CNT (Refs. 4 and 5) were reported. Also ratchet pumping through a multiwalled CNT was reported.⁶ Even though Talyanskii and co-workers^{4,5} and Ebbecke *et al.*⁷ reported the observation of current quantization on their specific device, the experimental results are not as clear as those reported in QPC based devices.¹ The difficulty of making a successful pump device utilizing CNTs arises from the fact that they are far from ideal. Spurious QDs may form from unavoidable CNT defects, impurities, and trapped charges on substrates. In this letter, we describe the observation of both the current quantization in Coulomb blockade (CB) state and the polarity change in the induced current at the CB peak by tuning the QD with different charging energies in the same QD-embedded CNT device. The polarity change in the induced current around the CB peak was observed when the charging of the QD was set to be around 5 meV while current quantization was observed when the QD is set to have 50 meV of charging energy. Our result clearly shows that current quantization can be observed only when the charging energy of the QD is relatively

big in a QD-embedded single-walled CNT based device.

We have fabricated a SAW driven electron pump device utilizing a single-walled CNT on a quartz substrate, as it is shown in Fig. 1(a). The device is composed of a pair of interdigital transducers (IDTs) and a CNT transistor. In order to get a high quality CNT, we used a single as-grown CNT on a 36° y-cut quartz substrate. A single-walled CNT was grown by thermal chemical vapor deposition on a quartz substrate with the patterned growth method.⁸ The IDT has 50 electrode-pairs of a 7-nm/10-nm-thick Cr/Au bilayer. The width of each electrode was kept to 250 nm and the distance between each pairs of electrodes was ~ 1.5 μm corresponding to a resonance frequency of 2.2 GHz. To reduce unwanted rf coupling between the CNT transistor and the IDT,

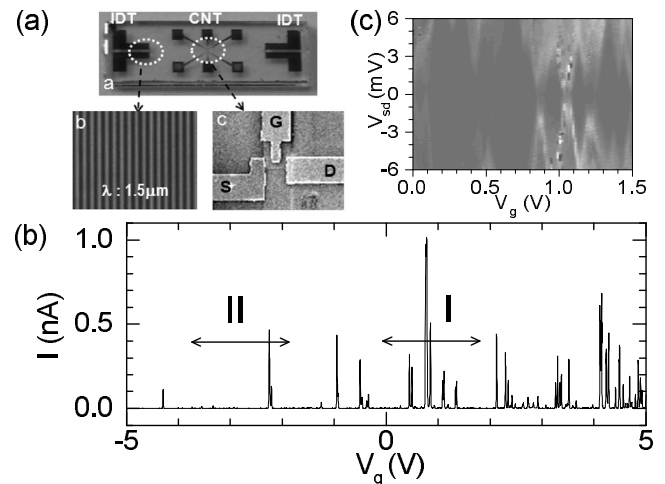


FIG. 1. (a) (Top) CNT transistor was fabricated in the middle of the device and two IDTs 2.5 μm away from the CNT transistor. (Left bottom) IDT with $\lambda = 1.5$ μm . (Right bottom) SEM image of a CNT transistor with a side gate denoted as G with channel length 1.5 μm . (b) Current (I) as a function of gate voltage (V_g) for bias voltage (V_{sd}) of 100 μV . I and II denote each region representing “small” charging energy and “large” charging energy for embedded QDs in a CNT, respectively. (c) dI/dV_{sd} density plot as a function of bias voltage V_{sd} and gate voltage V_g for $V_g = 0 - 1.5$ V belonging to region I. The brighter region represents higher conductance.

^{a)}Electronic mail: namkimfi@gmail.com.

the distance between the IDT and the CNT was kept 2.5 nm apart. The direction of a pair of the IDT is set to be aligned with the direction of the CNT. Electric contacts were made by depositing a 50-nm-thick Cr/Au film on top of a CNT with the diameter of 2 nm (which was confirmed by atomic force microscopy measurement). The distance between the source and the drain of the CNT transistor was about 1.5 μm , which corresponds to the wavelength of SAW. In order to minimize the attenuation of the SAW due to the conducting electrodes,⁹ we deposited a Cr/Au film as thin as possible. We used Agilent E8257D as the rf source whose frequency resolution is 0.01 Hz.

All the measurements were performed at 2.2 K. The two terminal resistance of the CNT was ~ 100 k Ω at room temperature. The CNT transistor showed CB oscillations, as evident from source-drain current versus side-gate voltage (I - V_g) curve. Figure 1(b) shows aperiodic CB oscillations in a wide range of V_g from -5 to 5 V, which may come from the multiple QDs formed by unintentional defects on the wire.¹⁰ The stability diagrams [Fig. 1(c)] of the devices were measured over the whole gate voltage range to estimate charging energies and the gate coupling constants α ($\alpha = C_g/C$ where C =total capacitance and C_g =gate capacitance) for each of the CB states. It has been found that the charging energy ranges from 5 to 60 meV depending on the gate voltages, and $\alpha \sim 0.05$. The CB states found in the range of gate voltages ~ 0 to ~ 2 V [denoted as region I in Fig. 1(b)] have charging energies of ~ 5 meV. On the other hand, the CB states in the range ~ -2 to ~ -4.5 V [denoted as region II in Fig. 1(b)] have charging energies of ~ 50 meV. From an empirical relationship $L[\text{nm}] \sim 1.4 \text{ eV}/E_c$ (where L is the length of the 1D QD and E_c is the QD charging energy) found by Bozovica *et al.*,¹¹ charging energies of 5 and 50 meV correspond to $L=280$ and 28 nm, respectively. Considering that the CNT channel length is ~ 1.5 μm , the calculated values seem acceptable. Nevertheless it cannot rule out the possibility of multiple quantum dots forming within the CNT. Thus, we believe that multiple quantum dots of different sizes formed due to the relatively long channel length. Aperiodic Coulomb oscillations can be interpreted simply as only one of the QDs is active while the other QDs are tuned to be transparent at certain gate voltages.¹² After measuring the charging energy of each CB state, we measured the SAW-induced acoustoelectric current through the device. We applied rf signals to an IDT at a resonant frequency with various rf-powers and measured the induced current through a CNT transistor when the source-drain voltage of the transistor is set to zero. We found that the SAW-induced current characteristic depends on the charging energy of CB states (depending on which QD is active).

Figures 2(a) and 2(b) show the SAW-induced current as a function of gate voltages and rf-powers for a QD with small charging energies (~ 5 meV). Figure 2(b) shows the SAW-induced currents measured when 0 and -5 dB m (dotted and dashed lines, respectively) of rf-power were applied to the IDT. For comparison, the CB peaks measured with 100 μV source-drain bias without a SAW was plotted as a solid line. It is clearly seen that the SAW-induced currents reverse their polarity at each Coulomb blockade peak. Also it can be noticed that positive and negative current peaks are separated out from a CB peak as the SAW power is increased. Figure 2(a) is the 2D density plot of the SAW-

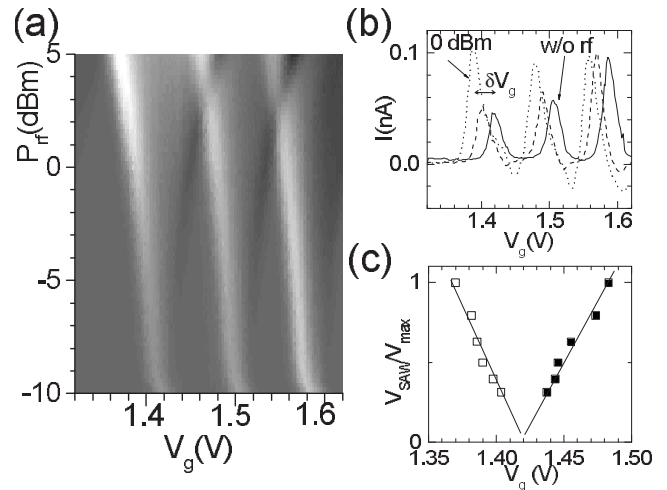


FIG. 2. (a) Current density plot as a function of rf-power P_{rf} applied to an IDT and gate voltages. (b) SAW-induced current (dotted line and dashed line for 0 and -5 dB m, respectively) and CBO without rf injection (solid line). δV_g denotes the shift of conductance peak in gate voltages. (c) Trace of conductance peaks (open square) and conductance dips (solid square) as a function of normalized SAW amplitudes and gate voltages.

induced current as a function of gate voltages and rf-powers P_{rf} (dB m) applied to an IDT. The figure clearly shows that the shift of the positive and negative current peaks depends on rf-power. Figure 2(c) shows the linear dependence of the peak shift as a function of normalized SAW amplitude ($V_{\text{SAW}}/V_{\text{max}}$) where V_{SAW} is proportional to $P_{\text{rf}}(\text{mW})^{1/2}$.¹³ These features are consistent with the so-called “double dot adiabatic pumping” model³ where one of the main results was the linear dependence of the peak shift as a function of V_{SAW} . The real SAW amplitude V_{SAW} (mV) can be estimated from Fig. 2(a). For instance, the rf-power of 0 dB m ($P_{\text{rf}} = 1$ mW) induces a peak shift $\delta V_g \sim 30$ mV in gate voltages. This value can be converted into real voltage scale by multiplying the side-gate coupling constant α (~ 0.05) estimated from the stability diagram analysis. This gives us the SAW amplitude V_{SAW} around 1.5 mV. From Fig. 2(a), it can be seen that the positive peaks and the negative peaks cross at $P_{\text{rf}} \sim 4$ dB m, which corresponds to 2.4 mV of SAW amplitude. This crossing roughly corresponds to half of a QD’s charging energy $E_c \sim 5$ meV. Since the positive and negative peaks are originating from different CB peaks, only a half of the charging energy is needed for them to crossover. When the SAW power is increased above this crossing point, other electron states become involved. Hence it is unreasonable to expect a current quantization.

Figure 3 depicts the results of SAW-induced current measured for a QD with a large charging energy (~ 50 meV). Since a relatively high rf-power is required to observe a current quantization, the measurements were done by applying pulse modulated rf signals to the IDT at a resonant frequency of 2.133 95 GHz to avoid unnecessary heating effects.¹⁴ The pulse modulated rf signal was set to 100 μs dwell time and 300 μs repetition time thus duty-cycle of 1/3. In order to observe current quantization, a CNT transistor was kept in a Coulomb insulator state (denoted by an arrow in the inset) by scanning the gate voltages from -2.32 to -2.28 V, which is slightly more negative than the CB peak position. The CNT channel was insulating in this gate voltage region with rf-power less than 0 dB m. Figure 3

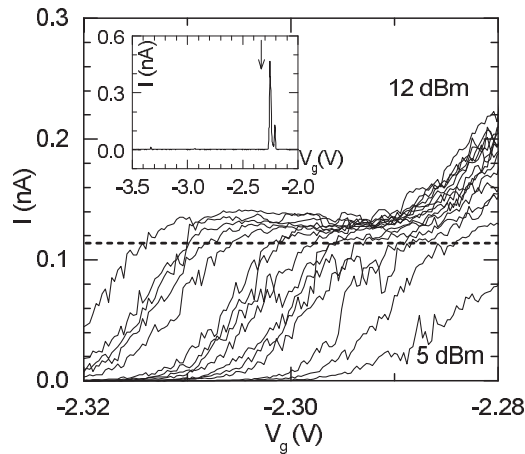


FIG. 3. SAW-induced current as a function of V_g for various rf-powers applied to transducers. The rf-powers were varied from 5 to 12 dB m by a 0.5 dB m step, and the frequency was set to a resonance frequency of $f_0 = 2.133\ 95$ GHz. The dotted line represents $ef/3 = 114$ pA where $1/3$ corresponds to the duty-cycle of the pulse modulated rf signal. The inset shows the CB oscillation curve without rf-power. The arrow denotes the Coulomb blockade region where the SAW-induced single electron pumping has been observed.

shows SAW-induced currents for various rf-powers. When the rf-power is increased from 5 up to 12 dB m, the threshold gate voltage is shifted to the negative direction and the induced current is increased. The induced current increases with the rf-power until saturated, resulting in a current plateau. We found that the current plateau was quite stable for certain gate voltages, bias voltages from -100 to $+100$ μV (not shown here), and certain range of rf-powers from 8 to 12 dB m. However, the value of current plateau is higher than $ef/3$ by ~ 20 pA, which is $\sim 20\%$ of the expected value. We would like to stress that the excess current is not due to the rectification effect since similar excess current with negative sign was also observed when the direction of the SAW was applied in opposite direction. The excess current is not due to any unwanted offset-bias to source or drain because the excess current was insensitive to the level of bias voltage from -100 to $+100$ μV applied between source and drain.¹⁵ We suspect that the discrepancy may be attributed to the different effective electron charges or strong correlations between electrons in a 1D wire (Luttinger liquid).¹⁶

In summary, we have measured SAW-induced currents through a QD-embedded single-walled CNT device for dif-

ferent QD charging energies. It is shown that the current quantization can be observed only when a QD has relatively a large charging energy while no current plateau was observed for a QD with a small charging energy (~ 5 meV).

We thank sample fabrication assistance from Sora Kim. This work was supported by the Korea Research Institute of Standard and Science. Y.C. was supported by the Korea Science and Engineering Foundation (KOSEF) grant funded by the Korea Government (MEST) (No. 2010-0000268). J.J.K. acknowledges the support from the National Research Foundation of Korea (R01-2008-000-11425-0).

- ¹J. Cunningham, V. I. Talyanskii, J. M. Shilton, and M. Pepper, *Phys. Rev. B* **62**, 1564 (2000), and references therein.
- ²V. I. Talyanskii, D. S. Novikov, B. D. Simons, and L. S. Levitov, *Phys. Rev. Lett.* **87**, 276802 (2001).
- ³M. R. Buitelaar, V. Kashcheyevs, P. J. Leek, V. I. Talyanskii, C. G. Smith, D. Anderson, G. A. C. Jones, J. Wei, and D. H. Cobden, *Phys. Rev. Lett.* **101**, 126803 (2008).
- ⁴P. J. Leek, M. R. Buitelaar, V. I. Talyanskii, C. G. Smith, D. Anderson, G. A. C. Jones, J. Wei, and D. H. Cobden, *Phys. Rev. Lett.* **95**, 256802 (2005).
- ⁵M. R. Buitelaar, P. J. Leek, V. I. Talyanskii, C. G. Smith, D. Anderson, G. A. C. Jones, J. Wei, and D. H. Cobden, *Semicond. Sci. Technol.* **21**, 569 (2006).
- ⁶Y.-S. Shin, W. Song, J. Kim, B.-C. Woo, N. Kim, M.-H. Jung, S.-H. Park, J.-G. Kim, K.-H. Ahn, and K. Hong, *Phys. Rev. B* **74**, 195415 (2006).
- ⁷J. Ebbecke, C. J. Strobl, and A. Wixforth, *Phys. Rev. B* **70**, 233401 (2004).
- ⁸J. Kong, H. T. Soh, A. M. Cassell, C. F. Quate, and H. Dai, *Nature (London)* **395**, 878 (1998).
- ⁹K. A. Ingebrigtsen, *J. Appl. Phys.* **41**, 454 (1970).
- ¹⁰P. L. McEuen, M. Bockrath, D. H. Cobden, Y.-G. Yoon, and S. G. Louie, *Phys. Rev. Lett.* **83**, 5098 (1999).
- ¹¹D. Bozovic, M. Bockrath, J. H. Hafner, C. M. Lieber, H. Park, and M. Tinkham, *Appl. Phys. Lett.* **78**, 3693 (2001).
- ¹²M. Bockrath, W. Liang, D. Bozovic, J. H. Hafner, C. M. Lieber, M. Tinkham, and H. Park, *Science* **291**, 283 (2001).
- ¹³It can be easily shown that $P_{\text{rf}}(\text{mW})^{1/2}$ is proportional to the SAW amplitude V_{SAW} because $P_{\text{rf}} = \beta P_{\text{SAW}}$ where β is the attenuation due to the impedance mismatching between coaxial line and IDT at a fixed frequency, and $P_{\text{SAW}}^{1/2}$ is proportional to the SAW amplitude V_{SAW} .
- ¹⁴M. Kataoka, C. J. B. Ford, C. H. W. Barnes, D. Anderson, G. A. C. Jones, H. E. Beere, D. A. Ritchie, and M. Pepper, *J. Appl. Phys.* **100**, 063710 (2006).
- ¹⁵The offset in bias voltage due to current amplifier or other sources was less than 70 μV . Also, the error of the uncalibrated current amplifier (Ithaco 1211) could not exceed 1% as we checked by comparing with other calibrated source.
- ¹⁶D. S. Novikov, *Phys. Rev. Lett.* **95**, 066401 (2005); R. Citro, N. Andrei, and Q. Niu, *Phys. Rev. B* **68**, 165312 (2003).